

N72-25357

LIDAR

R. T. H. Collis

Stanford Research Institute

ABSTRACT

Lidar is an optical 'radar' technique employing laser energy. Variations in signal intensity as a function of range provide information on atmospheric constituents, even when these are too tenuous to be normally visible. The theoretical and technical basis of the technique is described and typical values of the atmospheric optical parameters given. The significance of these parameters to atmospheric and meteorological problems is discussed. While the basic technique can provide valuable information about clouds and other material in the atmosphere, it is not possible to determine particle size and number concentrations precisely. There are also inherent difficulties in evaluating lidar observations. Nevertheless, lidar can provide much useful information as is shown by illustrations. These include lidar observations of: cirrus cloud, showing mountain wave motions; stratification in 'clear' air due to the thermal profile near the ground; determinations of low cloud and 'visibility' along an air-field approach path; and finally the motion and internal structure of clouds of tracer materials (insecticide spray and explosion-caused dust) which demonstrate the use of lidar for studying transport and diffusion processes.

Lidar is a generic, rather than a specific, technique and thus can be applied in a variety of forms to a wide range of research and operational problems. Research applications include: the investigation of dust in the high atmosphere; studies of air motion and turbulence revealed by cirrus and other clouds; boundary layer phenomena, as shown by variations in turbidity in the mixing layer; turbulence and diffusion processes using suitable indicators; and investigations of the effects of cirrus and other particulate

layers on measurement of radiation in and through the earth's atmosphere. Operational applications include: ceilometry, transmissometry, and the monitoring and tracking of atmospheric pollutants. Much progress is readily possible within the state-of-the-art, although higher pulse-rate lasers of higher average power are needed, together with the application of modern data-handling techniques and the development of quantitative methods of interpreting lidar data.

1. INTRODUCTION

The advent, in 1960, of the laser as a source of energy, opened up many possibilities for new techniques of probing the atmosphere or for improving and extending established techniques. The properties of this new form of energy were remarkable even at an early stage of technology. The energy, at optical or near optical frequencies was monochromatic, coherent, and, with the development of Q-switching techniques, could be generated in very short pulses of very high power. A number of scientists soon recognized the applicability of this device to atmospheric studies and described a variety of ways in which the special characteristics of laser energy could be exploited. These ranged from straightforward radar-type applications to more sophisticated concepts in which the wave nature and coherence of the laser energy were utilized. (See Schotland et al., 1962, Goyer and Watson, 1963, for example.)

The first actual use of lasers in atmospheric studies appears to be Fiocco and Smullin's use of a ruby laser "radar" to detect echoes from the atmosphere at heights up to 140 kms in June and July 1963. (Fiocco and Smullin, 1963.) At about the same time however, the late Dr. M. G. H. Ligda had initiated a program at Stanford Research Institute in which a similar pulsed ruby laser "radar" system, or lidar*, as Ligda called it, was used to probe the lower atmosphere and study meteorological phenomena. (Ligda, 1963)

Since that time, such simple 'radar' techniques have been applied by a number of workers to map and track concentrations of particulate matter and to study the density profile of the atmosphere by reference to gaseous backscattering. Meanwhile, others have been implementing some of the concepts involving the wave nature and coherence of laser energy. These include the use of multiple wavelength lidars to determine by reference to differential absorption the atmosphere's gaseous composition and also the use of Doppler techniques to determine motion in the atmosphere or, from molecular velocities, its temperature.

This paper will consider only the simple 'radar' approach and be concerned with the application of determinations of the intensity of backscattering of lidar energy to atmospheric studies and the solution of meteorological problems.

*The word lidar, an acronym analogous to radar, from Light Detection And Ranging, was earlier used by Middleton and Spilhaus (1953) in connection with pulsed-light ceilometers.

ILLUSTRATIONS SIGNIFICANT TO TEXT MATERIAL
HAVE BEEN REPRODUCED USING A DIFFERENT
PRINTING TECHNIQUE AND MAY APPEAR AGAIN IN
THE BACK OF THIS PUBLICATION

2. THE BASIC LIDAR TECHNIQUE

Energy generated by giant-pulse (Q-switched) lasers is highly monochromatic, essentially coherent, and is concentrated in very short, high-power pulses. This energy is directed by refracting or reflecting lens systems in a beam. Energy backscattered by the atmosphere within the beam is detected by an energy sensitive transducer (normally a photomultiplier tube) after being collected by suitable receiver lens systems. The monochromaticity of the energy makes it possible, by the use of narrow-band filters, to limit 'noise' in the form of energy of solar origin, to a minimum. The coherence of the energy makes it possible to achieve very narrow transmitter beams. A typical lidar system is shown in Figure 1; its characteristics are given in Appendix. (Northend et al., 1966)



Figure 1. MARK V 1967 Neodymium LIDAR

The essential features of lidar detection of atmospheric targets are described in the following equation:

$$P_r = \frac{P_t c \tau \beta' A}{8\pi r^2} \exp -2 \int_0^r \sigma(r) dr, \quad (1)$$

where

P_r is received power

P_t is transmitted power

LIDAR

- c is the velocity of light
- τ is pulse duration
- r is range
- β'_{180} is the volume backscattering coefficient of the atmosphere at range r (having dimensions of area/unit volume). (Following radar practice, β'_{180} is defined as an area that would intercept the same amount of energy as would yield the same return at the lidar if radiated isotropically at range r, as is, in fact, received from unit volume of the atmosphere at that range).
- A is the effective receiver aperture
- σ is the extinction coefficient

The basic lidar observation consists of an evaluation of received signal power P_r in terms of range and direction. The minimum detectable signal level is determined by either the system noise and that due to solar energy entering the receiver, or the sensitivity of the detector system. At laser wavelengths, even with systems of modest performance, the smallest hydrometeors may be readily detected, as well as the microscopic particles of the 'clear' aerosol.

It will be immediately apparent that unless the volume backscattering coefficient, β'_{180} , and the extinction coefficient, σ , are uniquely related, it is not possible to evaluate the intensity information in absolute terms. However, within certain limits the relationship between these parameters is sufficiently consistent to enable the significance of the variation of received signal with range to be unequivocal and of direct value. This is particularly the case where the lidar beam encounters strongly scattering targets after passing through relatively clear air, as occurs in observing clouds of particulates. Again, minor variations of signal intensity with range are immediately obvious and reveal layers and inhomogeneities in a continuously scattering atmosphere.

In practice, the signal from the photomultiplier is normally displayed on an oscilloscope as a function of range—the familiar A-scope presentation of radar practice. The single transient signal from a single shot may be photographed or magnetically recorded. Polaroid photography allows early inspection of the data in the former case, but the use of magnetic video disc memory makes a continuously viewable oscilloscope display available immediately as well as providing an input for more sophisticated analysis procedures and displays.

Although up to the present, data has largely been converted manually to punched cards or tape for subsequent computer processing and presentation, automatic data input techniques can readily be implemented. In the case of the very weak signals from high altitudes, where the signal is a function of the rate of generation of single photoelectrons, more sophisticated, automatic data processing techniques have already been employed (for example, McCormick et al., 1966, describe the on-line input of lidar data to a digital computer).

The limited data rate of the early lidar systems (with intervals between pulses measured in seconds if not in minutes) has restricted the resolution of observations in time,

and has precluded the development of scanning systems capable of developing two-dimensional sections of the type familiar in radar practice. (The lower data rate has perhaps been responsible for an earlier application of quantitative analyses than was the case with weather radar.) Both quantitatively and qualitatively however, lidar has made it possible to study remotely in three dimensions many atmospheric phenomena that hitherto could only be observed grossly or examined piecemeal.

3. ATMOSPHERIC OPTICAL PARAMETERS

Electromagnetic energy incident upon a volume of atmospheric gases and the liquid and solid particles suspended therein is scattered and absorbed. The magnitude of these effects is dependent upon the size and number of the particles present and their refractive index (and in this context gaseous molecules may be considered as particles) and also upon the wavelength of the incident energy. (In the case of laser energy, its highly monochromatic nature is an important consideration, for as shown by Twomey and Howell, (1965) the effects of critical wavelength/particle-size ratios are not averaged out so readily as is the case with broadband light sources.)

Of the energy scattered, that which is returned in the direction of the lidar, is evaluated in terms of the volume backscattering coefficient, β'_{180} (ℓ^{-1}). Energy removed from the direction of propagation, either by scattering or by absorption, can be evaluated most conveniently in terms of the extinction coefficient σ (ℓ^{-1}). This in turn can be considered in terms of the extinction due to scattering, σ_s , and the extinction due to absorption, σ_a . The important scattering and absorption mechanisms are now discussed.

3.1 Rayleigh Scattering

Rayleigh scattering from the molecular atmosphere is important for it provides a method by which atmospheric densities may be derived from lidar measurements. In addition, it also provides a convenient datum, to which other scattering and absorption effects may be related, in the upper atmosphere, particularly where layers of purely gaseous composition can be identified.

For wavelengths well separated from the absorption lines of the atmospheric constituents, the Rayleigh scattering cross section C_{RAY} of an individual scattering center is given (Van de Hulst, 1957) by:

$$C_{\text{RAY}} = \frac{8\pi}{3} \left(\frac{2\pi}{\lambda}\right)^4 \alpha^2 \frac{6 + 3\delta}{6 - 7\delta}, \quad (2)$$

where

λ = wavelength of incident radiation

δ = depolarization factor due to the anisotropy of the atmosphere

α = molecular polarizability of scatterer

LIDAR

For the atmospheric gases, the factor δ has a value near 0.035; therefore the fraction $(6 + 3\delta)/(6 - 7\delta)$ is about 1.061. The polarizability α is approximately $2 \times 10^{-30} \text{ (m}^3\text{)}$, and thus:

$$C_{\text{RAY}} = 3.96 \times 10^{-56} \lambda^{-4} \text{ (m}^2\text{)} \quad (3)$$

and at the ruby wavelength $\lambda = 0.694\mu$, for example,

$$C_{\text{RAY}} (\lambda = 0.694\mu) = 1.71 \times 10^{-31} \text{ (m}^2\text{)}. \quad (4)$$

The total scattering cross section per unit volume of a purely gaseous atmosphere is this elementary cross section multiplied by the number density N of molecular scatterers per unit volume.

$$\sigma_{\text{RAY}} + N C_{\text{RAY}} \quad (5)$$

This quantity σ_{RAY} is also called the Rayleigh attenuation coefficient. It is that quantity which, when multiplied by the incident power density and the effective illuminated volume, gives the total power scattered in all directions from the incident radiation beam.

For pure Rayleigh scattering it can be shown that $3/8\pi$ per steradian of this total will be scattered back toward the source. As a result of the convention used in defining radar cross sections (see Sec. 2 above) it follows that for Rayleigh scattering the volume backscattering cross section β'_{180} , can be obtained from:

$$\beta'_{180 \text{ RAY}} = 4\pi \frac{3}{8\pi} N C_{\text{RAY}} = 1.5 \sigma_{\text{RAY}} \quad (6)$$

Thus the factor k , which is the ratio of backscattering, β'_{180} , the extinction coefficient, σ , is for Rayleigh scattering a trusted constant (3/2) and not subject to the fluctuations encountered when the scattering particles become large compared to the wavelength. The significance of the value, $\beta'_{180 \text{ RAY}}$ in determining the density of the upper atmosphere is indicated in Table I.

Table I lists values for N from the U.S. Standard Atmosphere, 1962 (U.S. Government Printing Office, 1962) and for $\beta'_{180 \text{ RAY}}$ for sea level to 20 km elevation in 5 km increments.

Table I. Volume scattering coefficients for Rayleigh component of atmospheric scattering for ruby LIDAR ($\lambda = 0.6943\mu$)*

Height (km)	N (m^{-3})	β'_{180} (m^{-1})	σ_{RAY} (m^{-1})
0	2.55×10^{25}	6.55×10^{-6}	4.37×10^{-6}
5	1.52×10^{25}	3.93×10^{-6}	2.62×10^{-6}
10	8.60×10^{24}	2.21×10^{-6}	1.47×10^{-6}
15	4.06×10^{24}	1.04×10^{-6}	$.69 \times 10^{-6}$
20	1.85×10^{24}	4.75×10^{-7}	3.2×10^{-7}

*Rayleigh scattering is proportional to λ^{-4}

3.2 Mie Scattering

Mie scattering is of far greater significance than Rayleigh scattering in the lower atmosphere. It applies to particulate matter having dimensions of magnitude similar to the wavelength of the incident radiation. For large particles the elementary scattering cross section C_{MIE} is of the order of twice the geometrical cross section. The scattering pattern in the Mie case does not resemble the symmetrical-dipole pattern of Rayleigh scattering, but can be quite irregular and complicated (Middleton, 1953; Van de Hulst, 1957; Deirmendjian, 1964). The ratio of the backscattered to the total scattered energy is thus highly variable as a function of the particle-size to wavelength ratio and the dielectric characteristics of the particle. This is illustrated in Figure 2 which shows the relationship between backscattering and total scattering and the size parameter, α , for single spherical particles having a real refractive index of 1.33 (i.e., that of water). (The size parameter $\alpha = 2\pi a/\lambda$ where a is the radius.)

It will be seen that neither backscattering nor total scattering show significant general dependence on wavelength or particle size. Usually Mie scattering is predominantly forward so that in an assemblage of particles of different sizes, k , in the relation $\beta'_{180} = k\alpha$, is often less than unity. Because the effects of particle size differences tend to average out in such assemblages, useful approximate values can be determined for k and used in evaluating the lidar signal. Stanford Research Institute calculations for water sphere distributions typical of natural water clouds give an average value of $k = 0.625$. This value, together with the Attenuation Coefficients given in Elterman's Clear Standard Atmosphere (Elterman, 1964), have been used to compute values for the aerosol contribution to total backscattering for various altitudes as plotted in Figure 3. (The value $k = 0.625$ is most accurate for water spheres, but is a reasonable approximation for other aerosol components.)

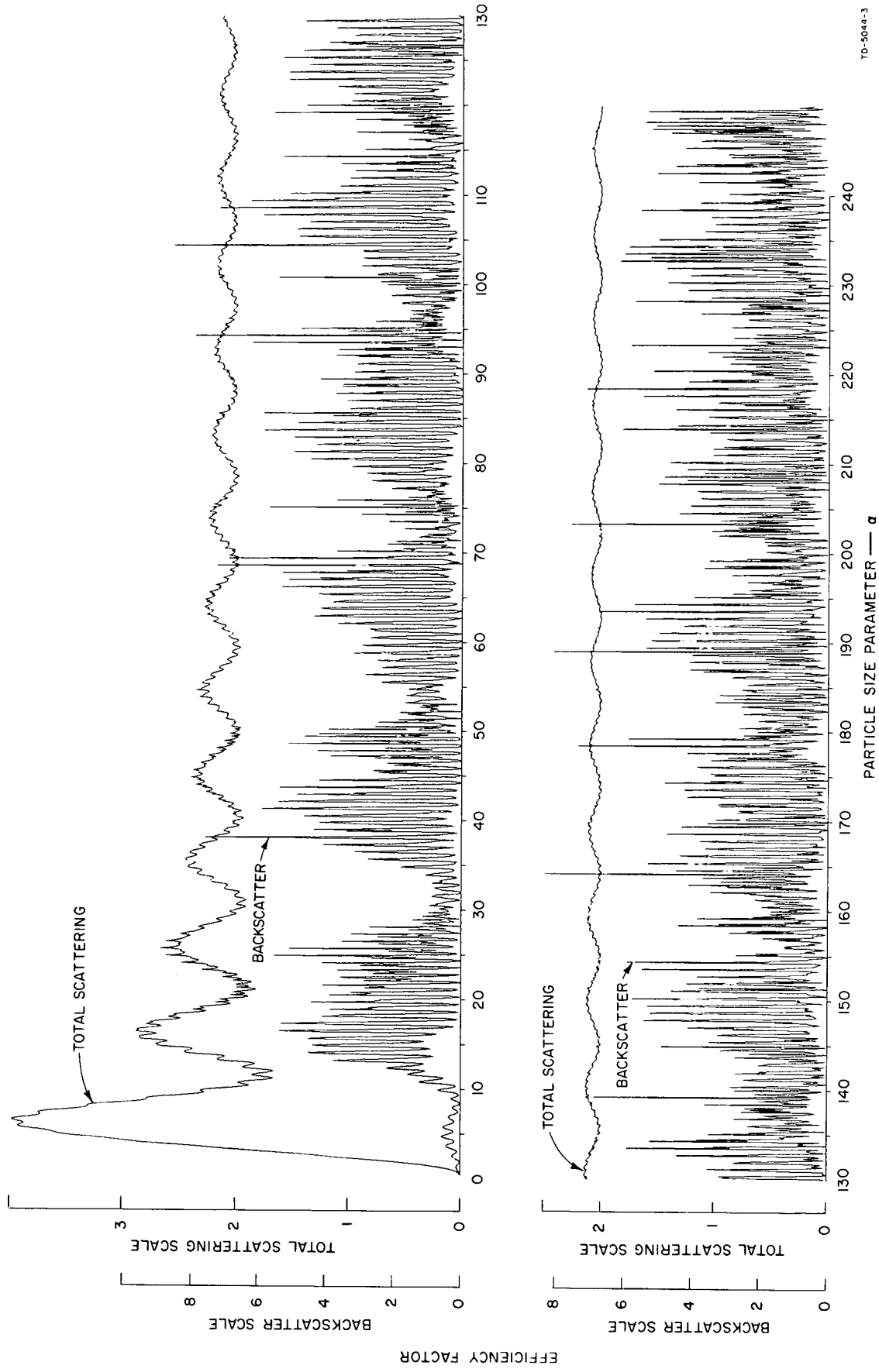
From this figure it is apparent that even on "clear" days (i.e., those with a horizontal visibility of about 25 km at sea level for the Elterman model) the aerosol backscattering predominates over the molecular backscattering for all elevations below 4 km.

Table II lists a range of typical water-cloud and haze conditions, together with the associated computed aerosol extinction coefficients, and anticipated volume backscatter coefficients, β'_{180} , under the assumption that $k = 0.625$.

Note however the generalizations involved in these examples (see Sec. 4 below).

3.3 Backscattering by Atmospheric Turbulence

The possibility of directly detecting atmospheric turbulence by lidar as a function of backscattering by dielectric inhomogeneities has attracted some attention. Among others, Munick (1965) has shown however, that this mechanism is far too feeble to encourage any hopes in this direction. For temperature and molecular number density values typical of altitudes of 10 km and a large temperature structure coefficient (representative of turbulent conditions near the ground), he shows that the backscattering due to turbulence at ruby wavelengths would be some 7 orders of magnitude less than that due to molecular backscattering!



TD-5044-3

Figure 2. Scattering efficiency factor as function of particle size parameter (refractive index: 1.33). Efficiency factor is ratio of respective scattering cross section to geometric cross section.

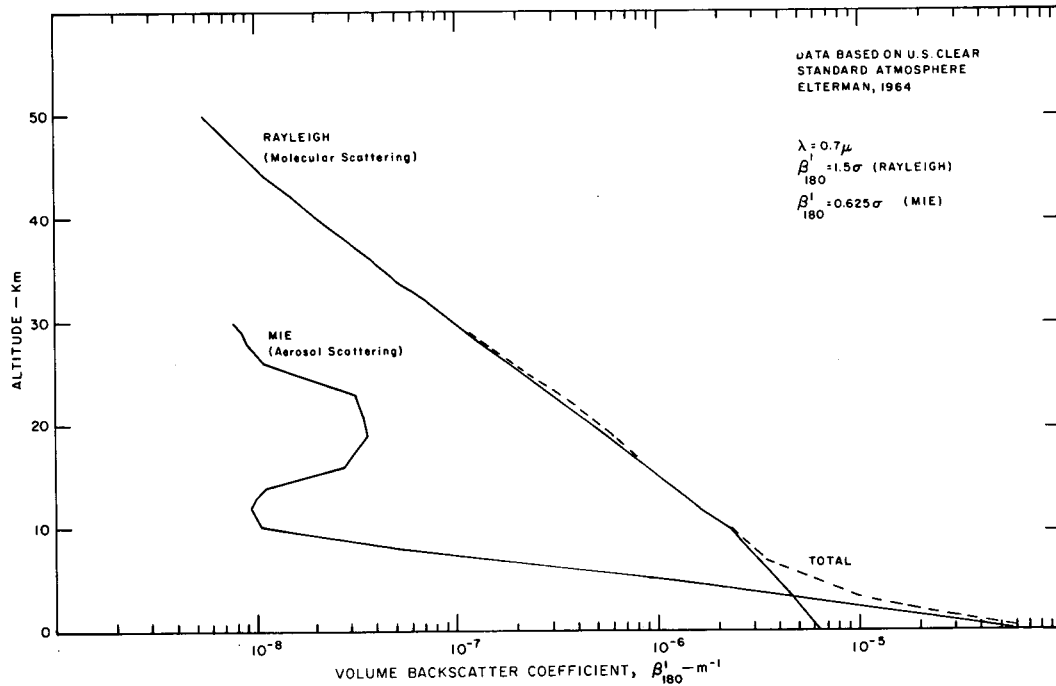


Figure 3. Volume backscatter coefficients for a clear standard atmosphere (for Ruby Lidar $\lambda = 0.6943 \mu$) Based on U.S. Clear Standard Atmosphere (Elterman, 1964). Note that a recent revision (Elterman, 1968) indicates a substantially larger aerosol content above approximately 4 km. The total backscattering profile based on these data would have the same general characteristics but would have values larger by a factor of approximately two above about 4 km up to the 30 km level.

Table II. Predicted volume backscatter and extinction coefficients for water clouds and hazes. For Ruby Lidars ($\lambda = 0.6943 \mu$) ($k = 0.625$)

	σ_{MIE} (m^{-1})	$\beta'_{180 MIE}$ (m^{-1})
Dense Water Cloud	3.2×10^{-1} to 1.6×10^{-2}	2×10^{-1} to 1×10^{-2}
Light Water Cloud	1.6×10^{-2} to 4.0×10^{-3}	1×10^{-2} to 2.5×10^{-3}
Thick Haze	4.0×10^{-3} to 1.1×10^{-3}	2.5×10^{-3} to 7×10^{-4}
Moderate Haze	1.1×10^{-3} to 4.8×10^{-3}	7×10^{-4} to 3×10^{-4}
Light Haze	4.8×10^{-3} to 1.6×10^{-4}	3×10^{-4} to 1×10^{-4}

3.4 Absorption

In addition to scattering, the gaseous atmosphere, and to a certain extent the industrially polluted aerosol absorbs energy. The attenuation due to this is generally insignificant in comparison to scattering losses, and $\sigma_{total} \approx \sigma_s$. Absorption is, of course, highly wavelength-dependent (especially at absorption line centers as exploited in spectroscopic lidar techniques), but may be neglected for many purposes in the basic

lidar application. Since in the operation of ruby lasers, heating can result in emission at the water vapor line centered on $.69438 \mu$ where the attenuation rate is some five times greater, some workers have found it desirable to control the laser operating temperature to avoid this (Kent et al., 1967).

4. THE SIGNIFICANCE OF LIDAR MEASURED OPTICAL PARAMETERS

4.1 Meteorological Significance

It is important to recognize that the magnitudes of the coefficients discussed above, and the relationships between the volume backscattering coefficients and attenuation coefficients are by no means absolute. They are given merely to provide general orders of magnitude and illustrate the relationships between the parameters in question.

For many meteorological and atmospheric applications, number and size spectrum of the aerosol particles is all-important. Although in certain cases, e.g., the measurement of visibility, the evaluation of the optical parameter as such, in this case the extinction coefficient, σ , will have direct significance. The quantitative contribution that lidar observations can make to meteorological studies is limited by the degree to which the optical parameters can be interpreted in terms of atmospheric characteristics.

Thus, in the case of the higher atmosphere, i.e., above 30-40 km, if the absence of particulate material can reasonably be inferred from the data, an evaluation of the volume backscattering coefficient is essentially a direct method of measuring atmospheric density. (Kent et al., 1967, Sandford, 1967). In 'clear' air in which particulate matter is present, the volume backscatter coefficient and the extinction coefficient can only be related to the particulate loading of the atmosphere within certain limits. Barrett and Ben-Dov (1967) discuss these in connection with lidar applications in air pollution measurements. They show that variations in assumed aerosol distribution parameters will produce relatively small errors (less than a factor of 2) in evaluation of particle concentrations from volume backscatter coefficient determinations.

While this degree of accuracy may be acceptable in air pollution studies, for other purposes it is obviously too uncertain. Fenn (1967) for example shows the limitations inherent in the relationship between atmospheric backscattering and the extinction coefficient in connection with the measurement of visual range. Twomey and Howell (1965 and 1967) also discuss the difficulties of deriving information on particle size distribution from optical measurements with special reference in their earlier paper to the monochromatic aspects of laser energy.

4.2 The Evaluation of Lidar Measured Optical Parameters

The discussion of the meteorological significance of optical parameters in 4.1 above has been carried on with the tacit assumption that the volume backscattering coefficients and the extinction coefficient can be evaluated. As noted in Section 2, the separation and evaluation of these terms cannot readily be accomplished from lidar observations, for unless a unique relationship exists between the volume backscattering coefficient and the extinction coefficient the lidar equation is unsolvable. The difficulties discussed above

(4.1) in connection with the interpretation of the significance of optical parameters apply in an especially critical way to attempts to interpret the lidar equation. Particularly because of the monochromatic nature of the energy, (Twomey and Howell, 1965) the relationship between backscattering and total scattering in the Mie region - i.e., for the particle sizes commonly involved in atmospheric aerosols and such features as cloud and fog, is highly variable. For a single scatterer, a diameter variation of, say, 1/100 can change the backscattering coefficient by a factor of 20. Although the averaging that occurs in the case of a volume of multi-size particles tends to stabilize the relationship (k) between the volume backscattering coefficient and extinction coefficient (see Sec. 3) at single wavelength, uncertainties in the relationship remain. Analysis techniques that rely on assumptions of any specific value of k are consequently apt to be in error. The difficulty lies in the fact that, unlike weather radars, (particularly those of wavelength of 10 cm or longer) any significant backscattering of lidar energy by atmospheric targets involves considerable attenuation.

Various analytical techniques have been proposed. For example, where the atmosphere is homogeneous, the derivative of the logarithm of the range-corrected received signal with respect to range, yields the attenuation coefficient in absolute terms.

$$\frac{d \log_e P_r r^2}{dr} \equiv -2\sigma \quad (7)$$

Barrett and Ben-Dov (1967) in the appendix to their paper describe the derivation and solution of an integral equation based on the initial assumption of a specific value of k .

The authors point out the instability inherent in approaches of this type, but show how errors can usually be confined to reasonable limits. At Stanford Research Institute (SRI) a similar approach has been taken but has been developed in the following form.

The data from the lidar signature is reduced in terms of the atmospheric optical parameters in a form which is called the lidar S-function* defined as:

$$S(r) \equiv 10 \log \frac{P_r(r) r^2}{P_r(r_o) r_o^2} \equiv 10 \log \frac{\beta'_{180}(r) T_a^2(r)}{\beta'_{180}(r_o) T_a^2(r_o)} \quad (8)$$

*The concept of the S-function was developed from the Spatial Backscatter Function (SBF) previously used at SRI (See Sec. 5). The SBF was defined as:

$$SBF(r) = 10 \log \beta'_{180}(r) T_a^2(r) \quad (9)$$

where β'_{180} has dimensions of km^{-1} . The S-function has the advantage of being dimensionless.

LIDAR

where $T_a(r)$ = one-way atmospheric transmission

$$= \exp \left(- \int_0^r \sigma(r') dr' \right) \quad (10)$$

and r_0 is a reference range.

When the backscatter is related to the extinction by

$$\beta'_{180}(r) = k_1 \sigma(r)^{k_2} \quad (11)$$

the derivative of the expression for $S(r)$ yields a first-order, non-linear differential equation

$$\frac{d\sigma}{dr} - c_1 \frac{dS}{dr} \sigma - c_2 \sigma^2 = 0 \quad (12)$$

where $c_1 = 1/4.34 k_2$ and $c_2 = 2/k_2$. The transform $\eta \equiv 1/\sigma$ reduces the equation to linear form for which the solution may be written as:

$$\sigma(r) = \sigma(r_0) e^{c_1 S(r)} \left[1 - c_2 \sigma(r_0) \int_{r_0}^r e^{c_1 S(r')} dr' \right]^{-1} \quad (13)$$

where knowledge of $\sigma(r_0)$ is required for solution.

Even in the absence of complete solutions, it is noteworthy that, unlike much of the work on weather radar, quantitative approaches are being developed and utilized in handling and displaying lidar data. This is encouraging for it appears that this will lead to progress both in the analytical technique and in the exploitation of modern data processing and presentation resources.

5. APPLICATION OF LIDAR OBSERVATIONS TO METEOROLOGICAL PROBLEMS AND ATMOSPHERIC STUDIES

5.1 General

Techniques for remotely probing the atmosphere can be directed towards measuring the temperature, density or composition (in terms of water vapor, ozone or carbon dioxide) of its gases, or to delineating and identifying the nature of its particulate content. In addition, the motions of the atmosphere are also of concern - both in terms of wind motion and turbulence.

What can lidar observations accomplish in these areas?

Direct evaluations of the backscattering profile in the upper atmosphere are believed to be capable of providing information on density profiles with sufficient accuracy to show seasonal variations in molecular density, at least in the layer from 50 to 80 kms, (Kent et al., 1967 and Sandford, 1967). However the possibility of unexpected particulate intrusions and the difficulty of making accurate measurements of returns from the tenuous upper atmosphere, make this approach rather uncertain, and in any case, it cannot be used when there are low clouds.

Other direct applications include the detection of the presence, height, shape, and in certain cases, thickness of clouds or haze layers. The evaluation of the atmospheric optical parameters (β'_{180} and σ) can also be considered direct observations which provide descriptive information on the atmosphere and its structure.

Finally from the nature of atmospheric structure, observed in this way, it may be possible to infer the motion of the atmosphere which has given rise to such a structure. Motion, however, is most readily inferred by observing the displacement of recognizable natural features or specifically introduced indicator materials (e.g., smoke).

5.2 Illustrative Examples

The uses of lidar for these purposes can best be appreciated from the following illustrative examples. These are selected from a wide range of applications to demonstrate the salient features of lidar application to this context and show the current state-of-the-art.

5.2.1 Cloud and Cloud Structure

A good example of the use of lidar in a qualitative role is provided by observations made of cirrus cloud in the Owens Valley, California, early in 1966. (Collis et al., 1968). The SRI Mk. V Ruby Lidar (see Appendix for details) was located near Independence and used to make a series of observations in a vertical plane parallel to the direction of air flow. The objective was to observe the features and dimensions of waves caused by the Sierra range. Figure 4 shows an example of the cloud structure observed in this way. The readiness with which the length and amplitude of the waves can be evaluated is obvious. Note that lidar echoes were obtained at slant ranges over 20 km for cirrus cloud, in daylight with the relatively modest system. The limited data rate (1 pulse per minute) however, restricts the resolution of the cross section both in space and time. Atmospheric structure revealed in this and similar cross sections (even of sub-visible inhomogeneities) offer a new capability for studying atmospheric motion with possible implications in the study of turbulent motion. (See Lawrence et al., 1968 for a report of lidar observations associated with turbulence experienced by an aircraft.)

Of course, denser lower clouds can readily be mapped by lidar (Collis, 1965). More quantitative studies of cirrus clouds are also being carried out at SRI in connection with radiometric measurements such as those made by satellite. An example of quantitative data reduced from lidar observations is shown in Figure 5. (Manually extracted data is processed and presented by computer and automatic plotter. Quantitative data are available on punched tape for further manipulation). Data such as these are compared with satellite cloud photographs and upper air soundings. As a subsequent experiment, it is hoped to compare them with radiometric data acquired by the Nimbus satellite.

5.2.2 Inhomogeneity in the 'Clear' Air

Variations in the turbidity of what appears to the eye to be clear air may readily be determined by lidar. Figure 6 shows a time/height cross section made at Menlo Park, California in 1967 by making a series of vertical lidar observations over an extended period. The data in the form SBF values (see 4.2 above) show the stratification clearly.

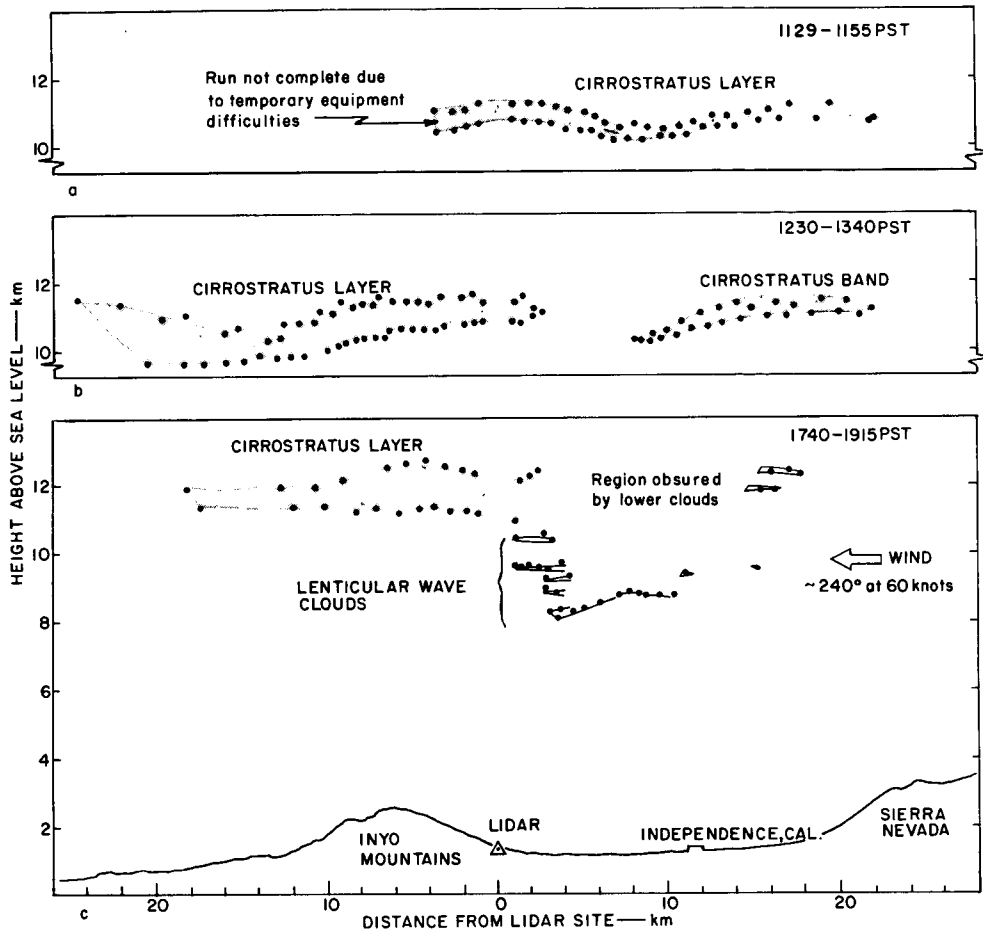


Figure 4. LIDAR observation of wave clouds in the lee of the Sierra Nevada, 1 March 1967. Data were obtained by scanning ruby lidar in the vertical and noting echoes at successive angles of elevation (indicated by data points).

The turbid air in the lower layer is separated from the overlying clean air at the level of the temperature inversion base (approx. 300 m). The transition layer between the turbid and clean air is marked in the illustration by the pair of lines roughly parallel to the time axis. This layer was particularly well defined during the period where the lines are heavy. The diurnal effects are apparent as relative humidity increased before sunrise, at which time vestiges of visible stratus cloud were observed to form.

Such lidar observations clearly offer contributions in observing and monitoring the effects of thermal stratification in the atmosphere and possible changes in its relative humidity. In addition, of course, remote quantitative observation may be made of the density of the particulate pollution loading and its changes with time (Barrett and Ben-Dov, 1967).

At higher levels, i.e., in the stratosphere and mesosphere, a number of workers have reported the detection of particulate layers, some of which are claimed to be associated with noctilucent clouds. (See Fiocco and Smullin, 1966; Fiocco and Grams, 1966; McCormick, P. D. et al., 1966; Collis and Lidga, 1966; Kent et al., 1967; and Sandford, 1967.)

5.2.3 Air Motion

If a suitable indicator or tracer material is injected into the atmosphere, lidar makes it possible to monitor its dispersal quantitatively and conveniently. For example, Figure 7 shows how a cloud of insecticide released by a low-flying aircraft moved down a wooded hillside, under the influence of air drainage. This example from observations made in Idaho in 1966 in connection with U.S. Forest Service studies of insecticide application shows the position of the cloud (which was quite invisible to the eye) along a fixed line of sight just above the tree tops at successive intervals of time. The velocity of the flow can readily be evaluated. In this case, the cloud remained fairly compact, but in other drops made under different meteorological conditions, the cloud dispersed rapidly. In such cases, especially as studied in a subsequent program conducted in 1967 (Figure 8) it was possible also to monitor the dispersal in the vertical, and by measuring changes in volume backscattering coefficient, to assess fall-out and diffusion (Collis and Oblanas, 1967).

Another example of transport studies is illustrated in Figure 9 which shows successive horizontal cross sections through a cloud of dust caused by an explosion in Montana in 1966 (Oblanas and Collis, 1967). These sections were made initially by allowing the cloud to drift through the lidar beam at successive fixed headings and thereafter by scanning in the horizontal plane. Even at the time of the dense first section, the dust suspension was too tenuous to be visible to the eye.

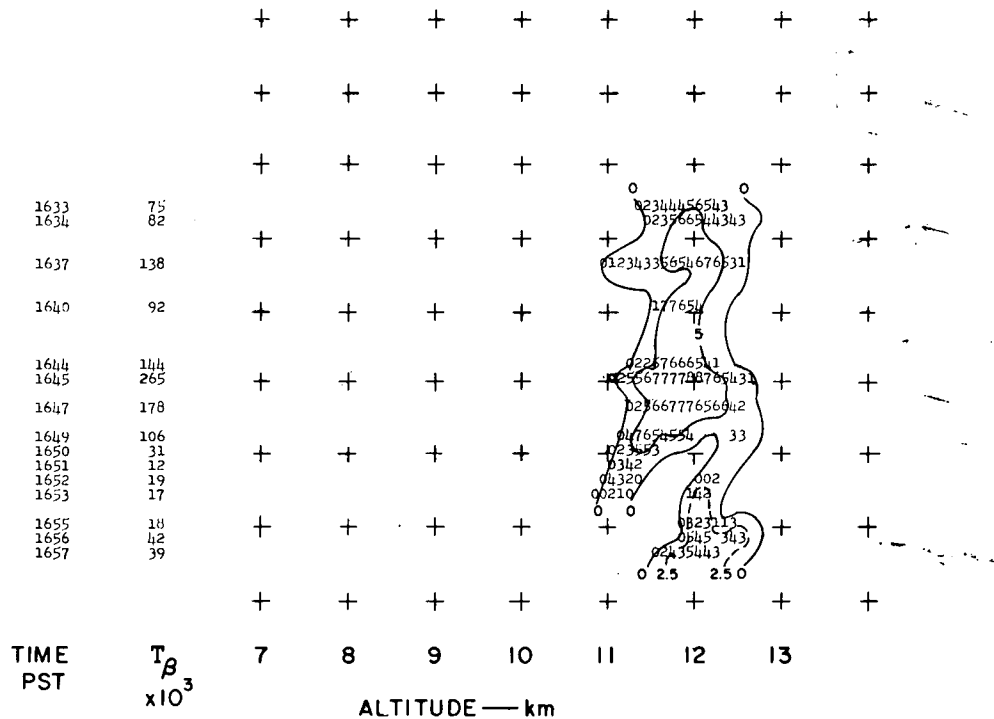


Figure 5. Graphical-quantitative representation of LIDAR cloud observations, Menlo Park, 8 December 1967. The automatically plotted data show volume backscattering coefficient values (for altitude increments of 100 m) expressed in a logarithmic code. The parameter shown as a number against each time indication similarly describes the transmission measured through the cirrus layer. Input data were manually reduced from Polaroid photographs.

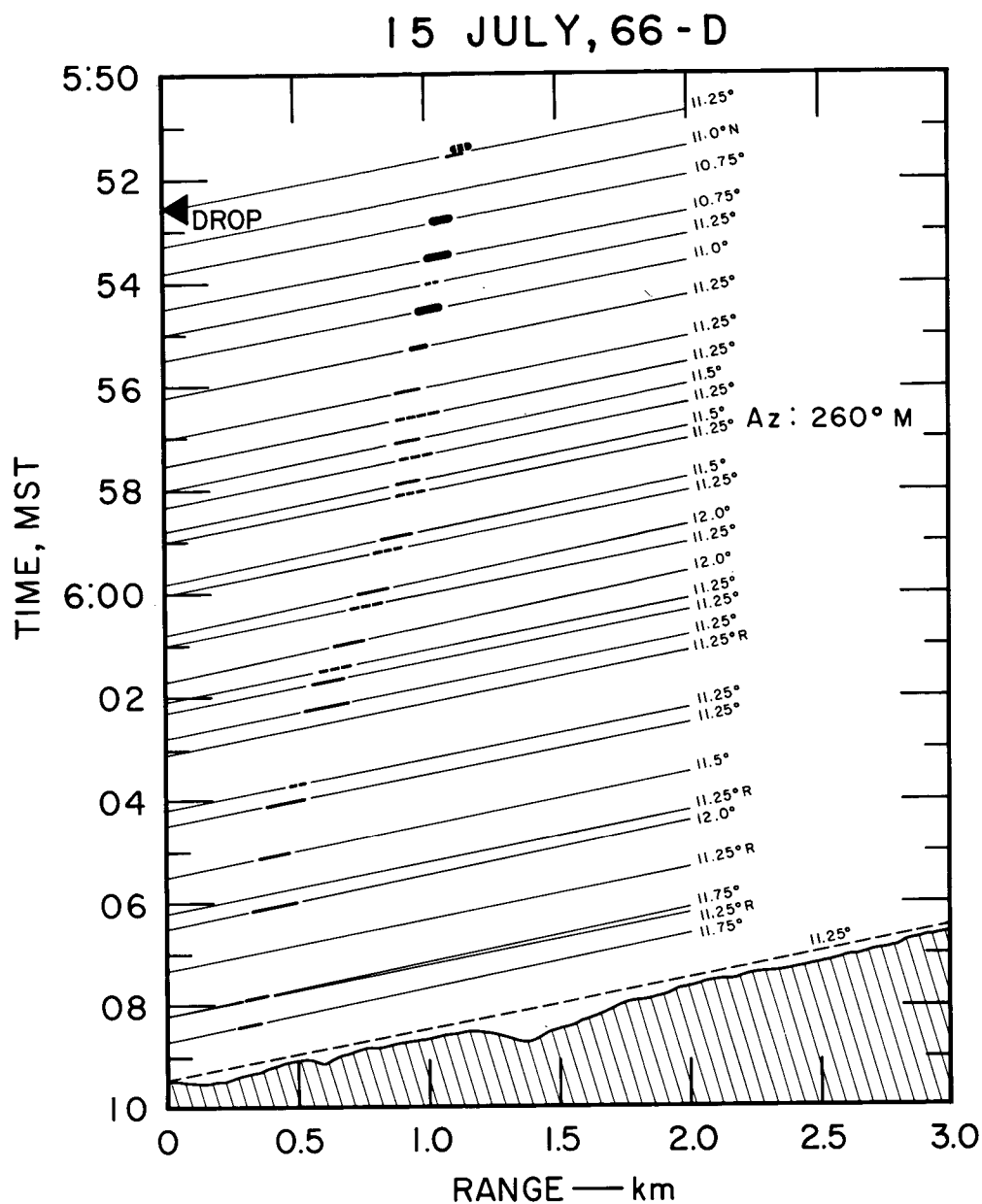


Figure 7. LIDAR observations of insecticide sprayed, by aircraft, Idaho, June 1966. Two lidars were used, ruby and neodymium. The echoes (continuous and dashed marks respectively) were detected in the positions shown at about the level of the tree tops (indicated by a dashed line). The insecticide was dropped at approximately 0552 MST (in concentration of 1qt/acre, droplet size of order 100 microns) from an aircraft flying about 60 m above the surface in a direction normal to the section represented. Note that the ordinate shows time and the diagram thus shows the results of lidar observations made at successive intervals as indicated. The insecticide was quite invisible to the eye.

LIDAR

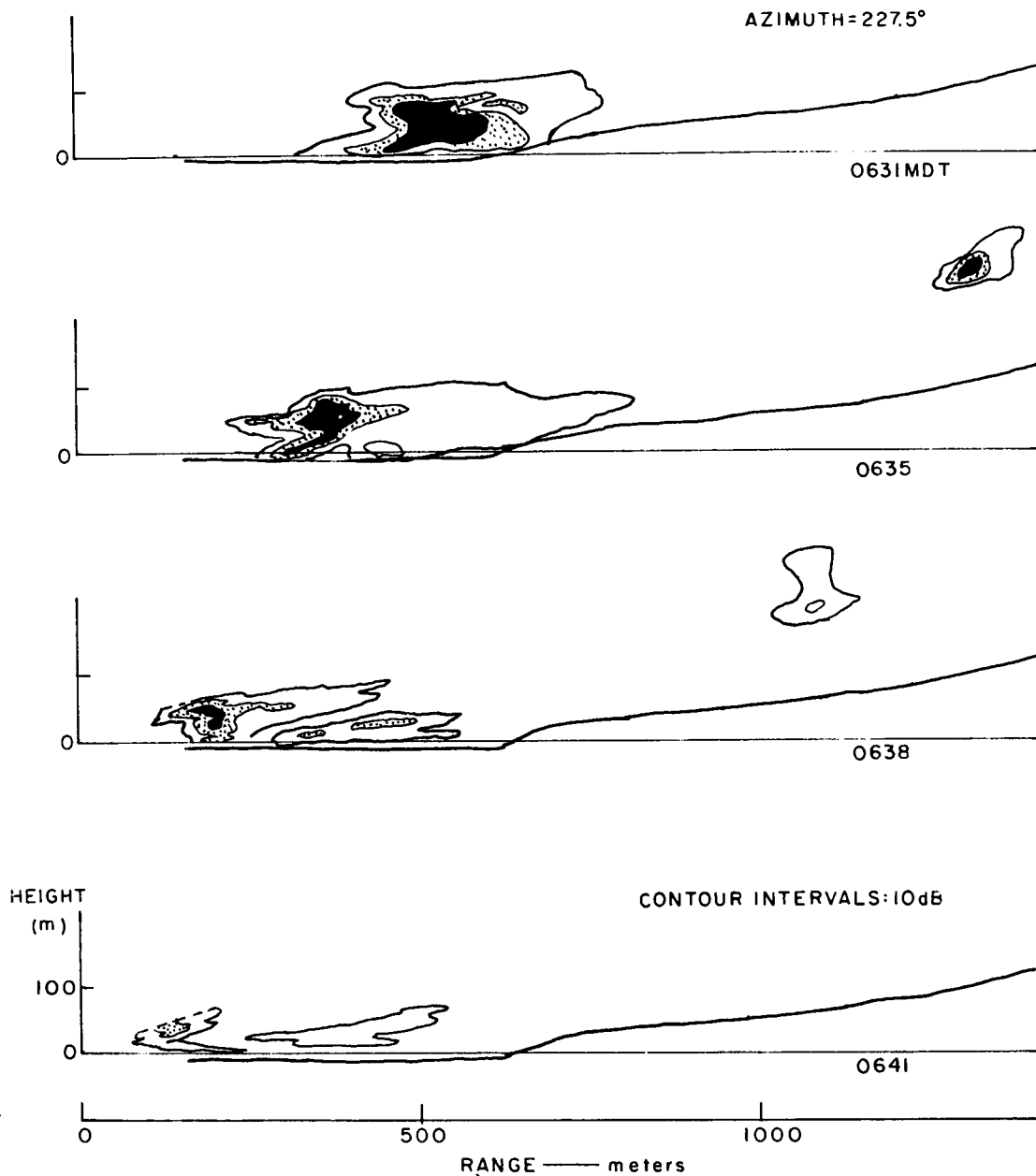


Figure 8. LIDAR observations of insecticide clouds, Idaho, June 1967. In this case a neodymium lidar was scanned in the vertical and observations were made at 1° intervals of elevation every 5 seconds. (The insecticide was sprayed in a similar manner to that described in Figure 7, but in this case the concentration was of the order of 0.5 pt/acre, with droplet sizes around 50 microns.) (The small cloud on the right of the illustration was smoke, also trailed by an aircraft.) The successive cross-sections (in which the internal structure is shown by relative backscattering coefficient isolines at 10 db intervals) show the motion and rate of dispersal of the insecticide (which was quite invisible to the eye).

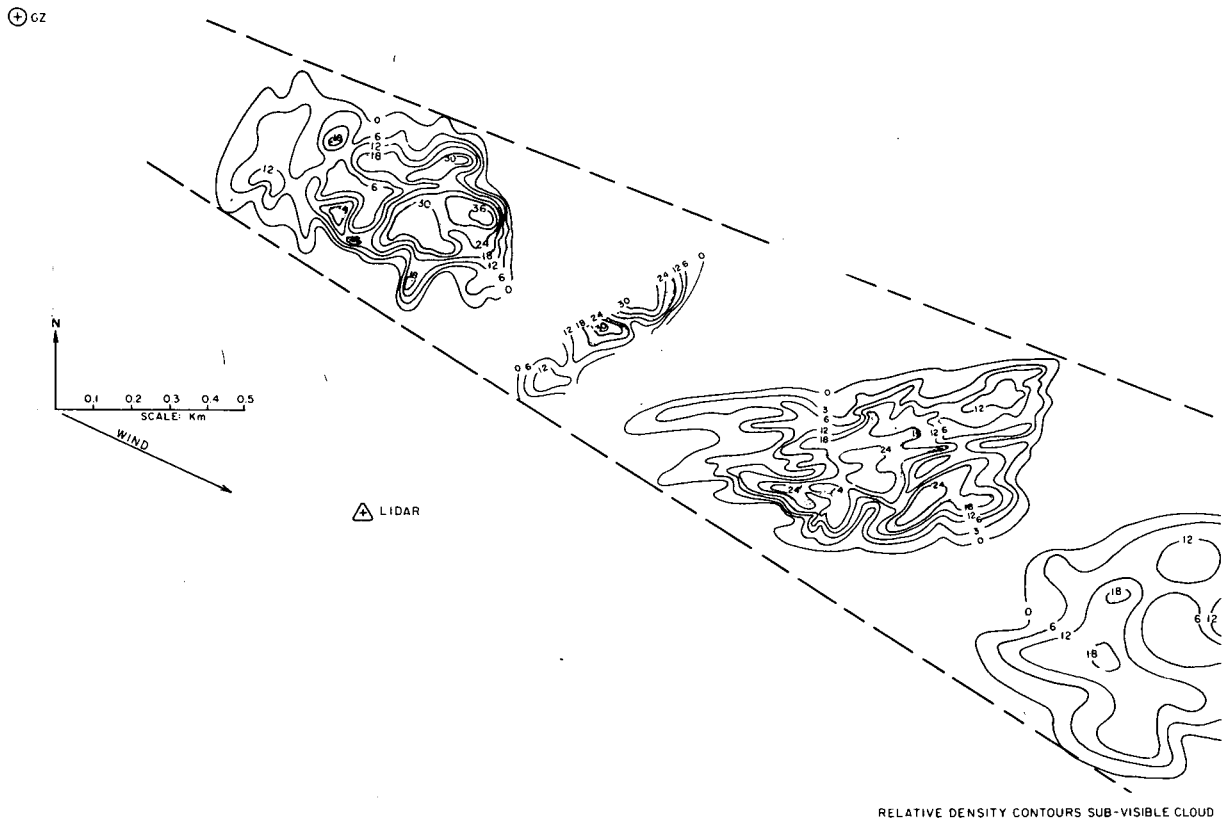


Figure 9. Series of four horizontal cross sections showing approximate relative density distributions of subvisible dust cloud. Cross sections were made with a neodymium lidar. (Observations time are centered at 3.0, 4.0, 6.0, and 8.3 minutes after the explosion which took place at Ground Zero (GZ) as indicated.) Dust was caused by the explosion of 20 tons of nitromethane at Fort Peck, Montana, November 1966. Even at the time of the first cross-section, however, no dust could be seen by the eye.

Similar sections have been made of explosion clouds using an airborne lidar (Collis and Oblanas, 1968) and work is continuing at SRI on applications of this type. Hamilton (1965) has also described lidar tracking observations of effluent from power station smoke stacks.

5.2.4 Fog and Low Cloud

A recent example of lidar observations of fog and low cloud is illustrated in Figure 10. It is of particular significance because it demonstrates the important contribution lidar can make in an operational role. At Hamilton AFB, California, the landing approach path on a well used runway lies over the waters of San Francisco Bay and adjoining marshes. The conventional rotating beam ceilometer located near the touch down point is only capable of monitoring cloud base immediately overhead. Conditions at this point are frequently not representative of conditions along the approach path. In experimental observations made with an SRI ruby lidar, the nature of the cloud base was monitored out along the approach to distances of up to 2 km in conditions of fog and low ceiling (visibilities of the order of 1000 m). The illustration shows a typical cross section

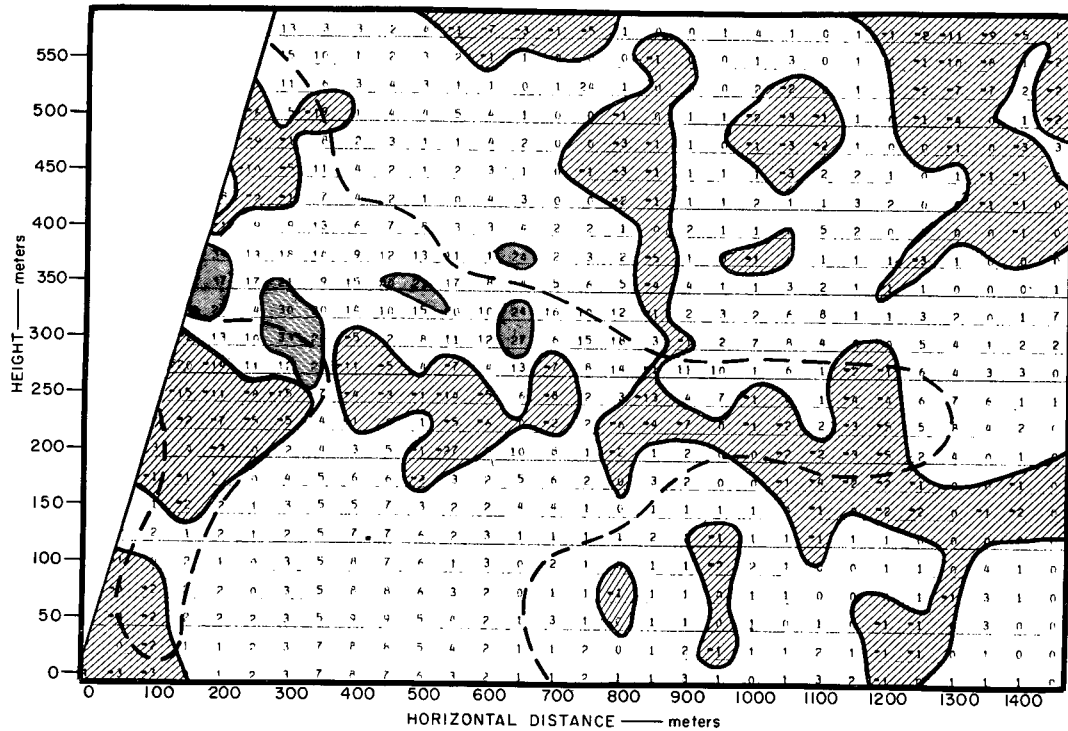


Figure 10. LIDAR observations of low cloud and reduced visibility conditions, Hamilton AFB, January 8, 1968. This is an analysis based on interim evaluations of extinction coefficient made by computer from manually entered data from a series of lidar observations. The parameter shown is σ (km^{-1}). Negative values show areas of rapidly increasing volume backscattering coefficient (i.e., dense cloud). Dotted line shows limit of area (i.e., within 700 m at the surface) of higher confidence in the data.

derived from a series of lidar observations scanning in the vertical. In addition to the delineation of the level of the diffuse cloud base, (c, 200 m) computations of quantitative parameters related to 'visibility' are shown over the section in question. Apart from the ability of lidar to observe cloud bases considerably displaced from its vicinity, this example illustrates the further potential of lidar for evaluating the important, but hitherto inaccessible operational parameter "slant visibility."

6. LIDAR CONTRIBUTIONS TO ATMOSPHERIC STUDIES AND METEOROLOGICAL PROBLEMS

It is important to recognize that the lidar technique applies broadly to a wide range of atmospheric and meteorological studies. We are dealing here with a generic rather than a specific technique.

The technique may be adapted and applied to a very diverse range of problems and it is hoped that these will be broadly evident from the above discussion and illustrations. The following seem particularly appropriate areas for lidar contributions:

General Research

1. Structure of dust layers in upper atmosphere, noctilucent clouds, etc. (20 to 150 km), atmospheric density (50-80 km).
2. Wave motion and turbulent air flow over orographic features and generally, as revealed by clouds and particulate inhomogeneities (at all levels up to say 15 kms).
3. Boundary layer structure (variations in low-level inversion levels, etc.) especially in relation to factors significant to air pollution in urban areas.
4. Turbulent mixing and diffusion processes, using indicator materials.
5. The effect of visible and sub-visible cirrus clouds and other aerosol layers on radiative transfer of energy within and through the atmosphere.

Operational

1. Ceilometry
2. 'Visibility' measurement, particularly over elevated slant paths for aircraft operations.
3. Wind profile measurement (using rocket disseminated trails of tracer material).
4. Tracking atmospheric pollutants from specific sources, e.g., insecticide spraying, nuclear tests, and smoke stacks.

7. FUTURE DEVELOPMENTS

Progress in the atmospheric and meteorological studies noted above (Sec. 6) could undoubtedly be made with little or no further technological development. There is much room for progress in the technological basis of the lidar technique, however. In certain fundamental aspects, advances in laser energy generation for example, progress will emerge as a result of new discoveries which can confidently be expected in this burgeoning field. In other aspects, many possibilities for progress are already readily apparent and achievable within the current state-of-the-art. The restrictive factors here are largely economic.

In the area of new developments, there is a need for higher repetition rate lasers providing higher average powers and higher data rates than are currently available. In this context, particularly for operational applications, eye safety considerations are important. Fortunately all requirements would be well met by a relatively low peak power with a high pulse repetition frequency, but it would be desirable in addition for such lasers to operate at wavelengths which are outside the visual range.

LIDAR

The development of high pulse rate lasers would lead to the development of systems capable of scanning in two dimensions to obtain nearly instantaneous atmospheric cross-section from stationary viewpoints, or more complete data from moving platforms such as aircraft or satellites. While such high-PRF systems would facilitate the development of graphical displays comparable to those used in weather radars, a more desirable development would be the input of such data to a computer for automatic quantitative processing and display. Techniques for handling data in this way are readily adaptable from currently available technology—but further progress must be made in developing techniques for recovering significant data from lidar operations.

Apart from the more obvious advantages of such data handling and presentation techniques, they open up the way to the powerful resources of modern information analysis procedures and the better coordination of lidar observations with other types of observations.

ACKNOWLEDGMENTS:

In preparing this review, I have drawn heavily upon the contributions of my colleagues at Stanford Research Institute and I am especially indebted to Dr. Warren Johnson, Dr. E. Uthe, and Mr. W. E. Evans for their assistance.

I am very conscious of having dealt only cursorily with the work of others elsewhere. Having relied mainly upon published descriptions of their work, my account is necessarily out of date in this respect.

Appendix

STANFORD RESEARCH INSTITUTE
TYPICAL LIDAR CHARACTERISTICS

	<u>Mark V</u>	<u>Mark I</u>
	<u>Transmitter</u>	
Laser Material	Neodymium-Glass	Ruby
Wavelength (μ)	1.06	.6943
Beamwidth (mrad)	0.2	0.5
Optics	6-inch Newtonian Reflector	4-inch Refractor
Peak Power Output (MW)	50	10
Pulse Length (ns)	12	24
Q Switch	Rotating Prism	Saturable dye
Max. PRR (pulses/min)	12 (1967) 1-2 (1966)	1-2
	<u>Receiver</u>	
Optics	6-inch Newtonian Reflector	4-inch Refractor
Field of View (mrad)(maximum)	3.0	2.0
Pre-Detection Filter		
Wavelength Interval (μ)	.01	.0017
Detector	RCA 7102 (S-1 Cathode)	RCA 7265 (S-20 Cathode)
Post-Detection		
Filter Bandwidth (MHz)	30	30

REFERENCES

- Barrett, E. W. and O. Ben-Dov, 1967: Application of LIDAR to air pollution measurements, J. Appl. Meteorology, 6, p. 500.
- Collis, R. T. H., 1965: LIDAR observations of clouds, Science, 144, p. 978.
- Collis, R. T. H. and M. G. H. Ligda, 1966: Note on LIDAR observations of particulate matter in the stratosphere, J. Atmos. Sc., 23, p. 255.
- Collis, R. T. H. and J. W. Oblanas, 1967: LIDAR observations of forest spraying operations, SRI Final Report, Contract 26-120, Forest Service, U.S. Dept. of Agric.
- Collis, R. T. H. and J. W. Oblanas, 1968: Airborne LIDAR observations-Pre Gondola II, U.S. Army Engineer Nuclear Cratering Group Report PNE-1119.
- Collis, R. T. H., F. G. Fernald and J. Alder, 1968: LIDAR observations of Sierra wave conditions, J. Appl. Met., 7, p. 227.
- Deirmendjian, D., 1964: Scattering and polarization properties of water clouds and hazes in the visible and infrared, Appl. Optics, 3, p. 187.
- Elterman, L., 1964: Atmospheric attenuation model, 1964, in the ultraviolet, visible and infrared regions for altitudes of 50 km, #46 Environmental Res. Papers, Air Force Cambridge Research Laboratories, AFCRL-64-740.
- Elterman, L., 1968: UV, visible, and IR attenuation for altitudes to 50 km, 1968, Environmental Res. Papers, No. 285, Air Force Cambridge Research Laboratories, AFCRL-68-0153.
- Fenn, R. W., 1966: Correlation between atmospheric backscattering and meteorological visual range, Appl. Optics, 5, p. 293.
- Fiocco, G. and L. D. Smullin, 1963: Detection of scattering layers in the upper atmosphere, Nature, 199, p. 1275.
- Fiocco, G. and Grams, 1966: Observations of the upper atmosphere by optical radar in Alaska and Sweden during the summer 1964, Tellus, 18, p. 34.
- Goyer, G. G. and R. Watson, 1963: The laser and its application to meteorology, Bull. A. Met. S., 44, p. 564.
- Hamilton, P. M., 1966: The use of LIDAR in air pollution studies, Air and Wat. Pollut. J., Pergamon Press, Oxford, Eng., 10, p. 427.
- Kent, G. S., B. R. Clemesha and R. W. Wright, 1967: High altitude atmospheric scattering of light from laser beam, J. Atmos. and Terr. Phys., 29, p. 169.

- Lawrence, J. D., M. P. McCormick, S. H. Melfi and D. P. Woodman, 1968: Laser backscatter correlation with turbulent regions of the atmosphere, App. Phys. Letters, 12, p. 72.
- Ligda, M. G. H., 1963: Meteorological observations with pulsed laser radar, Proc. 1st Conf. on Laser Technology, U.S. Navy, San Diego, Sept. 1963, p. 63.
- Long, R. K., 1963: Atmospheric attenuation of ruby lasers, Proc. IEEE, 51, p. 859.
- McCormick, P. D., S. K. Poultney, V. Van Wijk, C. O. Allen, R. T. Beltinger and J. A. Perschy, 1966: Backscattering from the upper atmosphere 75-160 km detected by optical radar, Nature, 209, p. 798.
- Middleton, W. E. K., 1958: Vision Through the Atmosphere, Univ. of Toronto Press.
- Middleton, W. E. K. and A. F. Spilhaus, 1953: Meteorological Instruments, Univ. of Toronto Press, p. 208.
- Munick, R. J., 1965: Turbulent backscatter of light, J. Opt. Soc. Amer., 55, p. 893.
- Northend, C. A., R. C. Honey and W. E. Evans, 1966: Laser radar (LIDAR) for meteorological observations, Rev. Sci. Instruments, 37, p. 393.
- Oblanas, J. W. and R. T. H. Collis, 1967: LIDAR observations of the Pre Gondola I Cloud, U.S. Army Engineer Nuclear Cratering Group, Report PNE-1100.
- Sandford, M. C. W., 1967: Laser scatter measurements in the mesosphere and above, J. Atmos. and Terr. Phys., 29, p. 1657.
- Schotland, R. M., A. M. Nathan, E. A. Chermack and E. E. Uthe, 1962: Optical sounding, Technical Report #2, New York University Report, Contract DA-36-039-SC87299, U.S. Army, E.R.D.L.
- Twomey, S. and H. B. Howell, 1965: The relative merit of white and monochromatic light for determination of visibility by backscattering measurements, Appl. Optics, 4, p. 501.
- Twomey, S. and H. B. Howell, 1967: Some aspects of the optical estimation of microstructure in fog and cloud, Appl. Optics, 6, p. 2125.
- U.S. Government Printing Office, 1962: U.S. Standard Atmosphere.
- Van de Hulst, H. C., 1957: Light Scattering by Small Particles, J. Wiley and Sons, New York, New York, p. 82.

PRECEDING PAGE BLANK NOT FILMED

COMMENTS ON "LIDAR" BY R. T. H. COLLIS

Earl W. Barrett
Atmospheric Physics and Chemistry Laboratories
ESSA Research Laboratories
Boulder, Colorado 80302

Dr. Collis has given an excellently clear and concise summary of the basic theory of lidar backscatter measurements, and of the various ways in which lidar data can be used in support of atmospheric research and meteorological observations. I cannot find any major points of disagreement with his presentation. My remarks are, therefore mainly concerned with emphasizing various points in his discussion which call most strongly for additional research and development. In the course of my remarks I will, however, occasionally give opinions which are sometimes more optimistic and sometimes more pessimistic than those which he has expressed.

My comments will fall into two general categories; those dealing with hardware problems and those dealing with evaluation, interpretation, and utilization of data.

I concur with Dr. Collis's statement that one of the most urgent needs is for lasers with high repetition rates, in order to avoid the necessity for photographic recording and subsequent tedious manual reduction of data. I believe, however, that unless the average output power can be increased by orders of magnitude, raising only the pulse rate will not allow the acquisition of any more information per unit time than is presently possible. For example, consider two lidars, one with a PRF (pulse repetition frequency) of 1 per second and a peak pulse power of 1 MW, and the other with a PRF of 1000 per second and peak power of 1 KW. I do not wish to pose as an expert on information theory, but it seems to me that the following argument holds: The signal-to-noise ratio, on a single shot, will be 30 db. poorer for the second lidar than for the first. It will therefore be necessary to average electronically 1000 pulses from the second lidar to establish the same S/N ratio. But this will require precisely one second, so that no time whatever will be saved.

What is really needed is a more efficient method of exciting the useful energy levels in solid-state laser materials. The present method of optical excitation with flashtubes is really a brute-force conversion of noise into information. As such, it is a statistically improbable phenomenon and therefore hopelessly inefficient. The average power of a solid-state laser is ultimately limited by two factors: The thermal conductivity of the rod material, and the surface-to-volume ratio of the rod. The first is beyond our

power to influence, so that only the latter is adjustable. The limit of improvement in this area has probably been reached already by use of fiber-optic bundles of doped glass, with interstices for coolant flow, in neodymium lasers. Hence the only hope for the future lies in finding better means of pumping. We thus have identified a prime research target.

With regard to choice of wavelength, it is evident that a compromise must be made with respect to various practical factors. A long wavelength reduces the Rayleigh and sky-light background, and is therefore desirable when aerosol or cloud measurements are the objective, but is contra-indicated for upper-atmosphere density measurements. Also, the efficiency of photodetectors falls off deplorably at wavelengths exceeding 1 micron, as do the transmittances and reflectances of lenses and mirrors. The multiplicity of absorption lines for water and CO₂ also introduce complications in data interpretation. At short wavelengths, sky-noise and Rayleigh background increase, and absorption by most atmospheric constituents sets in as the ultraviolet is approached. I therefore feel that the ruby wavelength represents the best possible compromise at present, with the neodymium running a close second (because of its higher possible PRF), if one is limited to a single general-purpose instrument.

The need for automation in the handling of lidar data is very apparent to anyone who has strained his eyes reading ranges and intensities to tenths of millimeters from Polaroid photographs of A-scopes. This is the rate-determining step in the entire process. In my own work on aerosols, the raw data are impressed on the film in one or two microseconds; the print is ready for inspection in 15 seconds, and is dry enough for handling in 15 minutes. Reading-off and tabulating some 30 significant levels from a print takes about an hour; punching these on cards consumes another half hour. The computer then finishes the job in about 1 1/2 seconds. Direct analog-to-digital conversion would save nearly two hours per sounding.

Dr. Collis's suggestion that a video magnetic recorder be used for storage and repetitive playback to a sampling-type digitizer is an excellent one in principle, but does have certain limitations, in my opinion. Video signals have a nominal bandwidth of 4 MHz, which implies a time resolution of the order of 250 nanoseconds or a range resolution of 125 feet. This may be adequate for some purposes, but certainly not for all. The matter of waveform distortion is also serious; what is adequate for playback of an entertainment video signal is, in most cases not sufficiently "high fidelity" for lidar work. Two sources of waveform distortion are easily identified. Although the DC component of a signal can be recorded on tape or disc, the playback is essentially a mathematical differentiation so that some low-frequency information is inevitably lost. Since any single-shot phenomenon, however short, has a spectral peak at zero frequency, it follows that some distortion will be introduced, in the form of a "sag" in the reproduced signal. Even though this may only amount to a few parts per million of the

peak amplitude, it may be unacceptably large in view of the 60-db dynamic range involved in a single lidar sounding. The other source of distortion is the variation in magnetic properties from point to point on the recording medium. I have not experimented with video recorders; I have, however, recorded a steady tone from a signal generator on a professional-quality audio tape recorder and observed 1-db fluctuations in level on playback. This would, in my opinion, be unacceptably large for quantitative lidar work. There is also ample chance for distortions of one or more per cent in the needed amplifications and signal mixings involved in magnetic recorders and playbacks. My philosophy is that, the less circuit elements between the photodetector and the Polaroid camera, the more reliable the information obtained.

Probably the most satisfactory arrangement would be real-time analog-to-digital conversion of the voltage appearing across the photodetector load resistance, followed by transfer of the digitized data to an on-line computer. The feasibility of this again depends on the range resolution desired. If one takes 25 feet as a target figure, the A-D conversion must be done every 50 nanoseconds; the 60-db dynamic range calls for 5-significant-figure digitization. I have not yet found any off-the-shelf system which will meet these requirements; my friends in the electronics profession are, in general, rather pessimistic about the possibility of meeting them in the near future. This is another research problem of pressing importance.

Turning now to the evaluation problems, I note that Dr. Collis's main point here is that the lidar equation is unsolvable unless the relationship between β'_{180} and σ , i. e., the backscatter and the total scatter, can be specified. I am in complete agreement with this statement. I believe, however, that he may be slightly too pessimistic when he states, on p. 157 of his paper that "----any significant scattering of lidar energy by atmospheric targets involves considerable attenuation." I have evaluated a number of soundings taken in rather dirty air, with and without the extinction term, and have found that in most cases the results differed by only a few per cent at the longer ranges. There are notable exceptions, particularly in stagnant maritime-tropical air under a subsidence inversion, when the error becomes as great as 50 per cent.

To illustrate this point, I have augmented Dr. Collis's Table II by computing some values of β'_{180} and σ (for the aerosol contribution alone) for my "standard aerosol", which has a radius range of 0.04 to 10.0 microns, a mass-median radius of 0.63 micron, is distributed in accordance with the Junge " r^{-3} law", and has an index of refraction of 1.5. Rather than categorizing the haze as light, moderate, or heavy, or by number density, I have used visibility (in the sense of Koschmieder) as the parameter. The basis for the calculation is the scattering table of De Bary et al (1965). The results are tabulated below.

TABLE I

Haze Scattering (Aerosol Component)

<u>V (mi)</u>	<u>β'_{180} (m^{-1})</u>	<u>σ (m^{-1})</u>
20	4.36×10^{-5}	9.00×10^{-5}
15	5.89×10^{-5}	1.21×10^{-4}
10	9.03×10^{-5}	1.86×10^{-4}
5	1.22×10^{-4}	2.51×10^{-4}
2	4.68×10^{-4}	9.64×10^{-4}
1	9.39×10^{-4}	1.93×10^{-3}
1/2	1.88×10^{-3}	3.88×10^{-3}

$$(\beta'_{180} = (943V^{-1} - 4) \times 10^{-6}, V \text{ in miles; } \sigma = 2.06\beta'_{180}, k = 0.486)$$

It is clear that, if the visual range is greater than 20 miles, the error made by dropping the extinction term in the lidar equation will be less than 18 per cent at a distance of 1 km. It has been my experience that, once one ascends above the polluted boundary layer, the subjective visibility is much greater than 20 miles in most meteorological situations (excluding clouds); it is usually 100 miles or more. This is confirmed by the lidar data at Chicago. For most vertical soundings, therefore, even a rough estimate of Dr. Collis's k will yield sufficiently accurate calculations of β'_{180} even at long ranges. For slant observations at low elevation angles in the boundary layer, or when one is stretching the capability of the technique by trying to measure quantitatively the aerosol concentration in the stratosphere, I agree that greater precision is required.

Dr. Collis's frequent reference to the work of Twomey and Howell, in pointing out the uncertainties in the proper value of k , brings me to my last main point. When I first saw their plot of ζ (Dr. Collis's k) as a function of particle radius for a wavelength of 0.7 micron, I was quite shocked. It struck me that the plot looked much more like noisy experimental data than like the solution of a neat mathematical model. I have not singled out these authors for special criticism; I have simply developed considerable skepticism about all computations based on the Mie theory. I do not mean to imply that the theory, as such, is unsound; I refer, rather, to the appallingly numerous opportunities for the entrance of computational noise when the usual algorithms (as I have seen them) are used. The scattered intensity (for each polarization) consists of the square of an infinite series of amplitudes, each multiplied by a function of the scattering angle. The convergence rate of this series is known to be very slow; the possibility of significant truncation error is therefore great. Furthermore, the individual amplitudes are each a ratio of differences of two numbers. These numbers, in turn, are products of Bessel functions, which are (I suspect) calculated in practice by means of recursion equations; this invites

cumulative error. I suspect that the major source of computational noise lies in those ratios of (possibly small) differences of (possibly large) numbers which occur in the amplitudes. In addition, when the scattering by polydisperse aerosols is to be computed, a numerical integration over the size distribution must be carried out. This smooths out irregularities, to be sure, but offers additional opportunity for quantitative error.

I feel, therefore, that further work must be done to recast the Mie algorithms into forms less sensitive to computational noise; probably by transformation to new variables. I have been spending considerable time recently on just this problem, with, however, a notable lack of success so far. I would like very much to enlist the aid of applied mathematicians in this, which I identify as the third major obstacle standing in the way of more effective utilization of the lidar.

With reference to the observation of Dr. Collis that the quantitative approach has entered rather earlier in the history of lidar than in that of radar, I agree that the low PRF of the lidar, which precludes the eye-catching but qualitative intensity-modulated areal displays, has been an important factor. I should like to suggest some possible other contributors. One of these is the considerable body of experience already acquired with radar. Another is the fact that meteorological uses of radar were first discovered during wartime, by military users, and were promptly slapped under tight security classification. Still another is the fact that, since lidar operates in or near the visible spectrum, the qualitative phenomena involved are already familiar to the eye and hence are less interesting and novel. Furthermore, the quantitative application of radar which was most obvious, and hence most studied, is the measurement of precipitation; the radar has had a much cheaper competitor in the rain gauge. As a converse proposition, many of the qualitative functions the lidar can perform can be done more cheaply by other means (such as ceilometers).

To Dr. Collis's list of present and prospective uses for the lidar, I would like to add one or two more. The water-vapor line at 0.69438 micron, which is a nuisance in most other applications of the ruby lidar, offers the possibility of remote humidity soundings by comparison of the returns from two lidars, one tuned inside the line and the other outside. I believe that Dr. Schotland will discuss this particular application in detail in his paper, so I will not say more. I will mention another effect of humidity which is also a bother in aerosol work, but which is helpful when the lidar is used to monitor the height of subsidence inversions. The sorption of water by hygroscopic and hydrophilic aerosol particles increases their sizes and hence their scattering cross-sections, as the humidity increases. The effect is to produce the analog of the "bright band" of radar meteorology, because the humidity normally reaches a maximum at the inversion base, while both the humidity and aerosol count decrease rapidly through the inversion.